

A growing string method for the reaction pathway defined by a Newton trajectory

Wolfgang Quapp^{a)}

Mathematical Institute, University of Leipzig, Augustusplatz, D-04109 Leipzig, Germany

(Received 1 December 2004; accepted 14 February 2005; published online 3 May 2005)

The reaction path is an important concept of theoretical chemistry. We use a projection operator for the following of the Newton trajectory (NT) along the reaction valley of the potential energy surface. We describe the numerical scheme for the string method, adapting the proposal of a growing string (GS) by [Peters *et al.*, *J. Chem. Phys.* **120**, 7877 (2004)]. The combination of the Newton projector and the growing string idea is an improvement of both methods, and a great saving of the number of iterations needed to find the pathway over the saddle point. This combination GS-NT is at the best of our knowledge new. We employ two different corrector methods: first, the use of projected gradient steps, and second a conjugated gradient method, the CG+ method of Liu, Nocedal, and Waltz, generalized by projectors. The executed examples are Lennard-Jones clusters, LJ₇ and LJ₂₂, and an N-methyl-alanyl-acetamide (alanine dipeptide) rearrangement between the minima C7_{ax} and C5. For the latter, the growing string calculation is interfaced with the GASSIAN03 quantum chemical software package. © 2005 American Institute of Physics. [DOI: 10.1063/1.1885467]

I. INTRODUCTION

The design of a robust method for the determination of a reaction pathway (RP) on a complex energy landscape is a very important problem. This work uses Newton trajectories (NTs) in double-ended methods of a recent paper of the author,¹ combined with a proposal of a growing string (GS) method recently given by Peters *et al.*² A RP of an adiabatic potential-energy surface (PES) is the usual approach to the theoretical kinetics of large chemical systems. The RP is any line connecting two minima by passing the saddle point (SP) in n -dimensional coordinate space. The energy of the SP is assumed to be the highest value tracing along the RP. It is the minimal energy a reaction needs to take place. We do not find it difficult to recognise RPs, we find it difficult indeed to offer a definition that is conceptually watertight and immune to counterexample.³ Here we use the distinguished or driven-coordinate method⁴ in the modern form of the reduced gradient following (RGF),^{5,6} also called NT. We insist that the search of an appropriate RP is not necessarily equivalent to the finding of the steepest descent from SP.⁷ Most RPs can be defined with the help of projection operators.¹ The tool is employed in string methods:^{8,9} the string is divided into a collection of nodes which are moved by projectors. The nodes $\mathbf{x}_1, \dots, \mathbf{x}_m$ represent the RP by a chain of length m , where the endpoints may be the minima \mathbf{x}_0 and \mathbf{x}_{m+1} .

Our GS-NT method is divided into predictor and corrector steps. We describe both, and especially the termination criterion and performance of the corrector, and at the very end, the implementation of two different methods for the corrector step.

II. NEWTON TRAJECTORIES

We define the projection operator. We choose an n -dimensional column vector \mathbf{r} for the projection. It has to be a unit vector. We additionally use the transposed vector \mathbf{r}^T being a row vector. The dyadic product $\mathbf{D}_r = \mathbf{r} \cdot \mathbf{r}^T$ is an $(n \times n)$ matrix. \mathbf{D}_r projects with \mathbf{r} :

$$\mathbf{D}_r \mathbf{r} = (\mathbf{r} \cdot \mathbf{r}^T) \cdot \mathbf{r} = \mathbf{r}(\mathbf{r}^T \cdot \mathbf{r}) = \mathbf{r}. \quad (1)$$

The projector which projects down the \mathbf{r} is with the unit matrix \mathbf{I}

$$\mathbf{P}_r = \mathbf{I} - \mathbf{D}_r. \quad (2)$$

The concept of RGF^{5,6,10} is that a selected gradient direction is fixed along the curve $\mathbf{x}(s)$, with curve parameter s for gradient \mathbf{g} of the PES

$$\mathbf{g}(\mathbf{x}(s)) / \|\mathbf{g}(\mathbf{x}(s))\| = \mathbf{r}. \quad (3)$$

Which direction \mathbf{r} to select is a certain arbitrariness.¹ We will discuss it below using some examples. The original driven-coordinate method⁴ employs the eigenvector direction of a reaction valley. However, in the (higher-dimensional) examples below, we will not execute the calculation of the Hessian at all.

The property (3) is realizable by a projection of the gradient employing \mathbf{P}_r of (2). We pose the Newton projector⁶

$$\mathbf{P}_r \mathbf{g}(\mathbf{x}(s)) = \mathbf{0}. \quad (4)$$

\mathbf{P}_r is an $n \times n$ matrix of rank $n-1$. The solution $\mathbf{x}(s)$ is named Newton trajectory. If starting at a minimum, Eq. (4) is trivially fulfilled for every direction \mathbf{r} . Thus, we may choose any direction because there is a solution which starts at the minimum. If starting at any point, we have to choose for \mathbf{r} the normalized gradient of the point. In the general good-natured case, each NT passes each stationary point. A full

^{a)}FAX: (49) 341-9732199. Electronic mail: quapp@rz.uni-leipzig.de

family of NTs connects the extrema if we vary the search direction \mathbf{r} ,¹¹ thus, NTs better connect saddle-dominated regions with minima-dominated regions than the steepest descent/ascent can do. A monotonely increasing energy profile over an NT, or a monotonely decreasing, as well, indicates a true, convex reaction valley.¹² Projector (4) can be used in a string method at every actual chain point, without any further derivative.¹ If it does not result in zero, choose the downhill direction of a node moving along

$$\mathbf{p} = -(\mathbf{I} - \mathbf{r} \cdot \mathbf{r}^T)\mathbf{g}. \quad (5)$$

The application of the projector does not need the tangent of the curve, any reparameterization of the string, nor any spring forces of the chain, and every chain point can be moved independently.¹ It predestinates the Newton projector for the growing string method² in an exceptional kind. The main problem under an application of operator (5) is nothing but finding an appropriate steplength or a dampening factor η for \mathbf{p} .

III. GROWING STRING METHOD

The growing string method adaptively evolves the string from its endpoint(s). Because the nodes grow along the RP, the string can avoid excessive rugged regions of a PES where electronic structure calculations may fail. We search a RP which should connect the initial minimum \mathbf{x}_{ini} with the end \mathbf{x}_{fin} by a chain of m nodes \mathbf{x}_k . We calculate successive nodes beginning at the initial minimum.

- (i) \mathbf{x}_k is an approximated node on the RP. We choose a next guess point, \mathbf{y}_{k+1} , of the string between the actual node and the final minimum by

$$\mathbf{y}_{k+1} = \lambda \mathbf{x}_k + (1 - \lambda) \mathbf{x}_{\text{fin}}, \quad \lambda = \frac{m - k}{m + 1 - k}, \quad (6)$$

$k=0, \dots, m-1$, see Fig. 1, where m is the desired number of nodes and $\mathbf{x}_0 = \mathbf{x}_{\text{ini}}$, $\mathbf{x}_{m+1} = \mathbf{x}_{\text{fin}}$.

- (ii) Doing corrector steps with the gradient at the guess point \mathbf{y}_{k+1} using the Newton projector (5) up to convergence, thus up to a threshold ϵ for the right side of (4), see Fig. 1, the steps go orthogonally to the search direction. In this paper we use two different corrector methods: first, the pure Newton projector with an appropriate dampening factor η and second, a conjugate gradient method modified by the Newton projector.
- (iii) The point at convergence is the next node, \mathbf{x}_{k+1} , and the process is repeated up to the final minimum.
- (iv) If more than one SP is found on the chain, one may adapt the search direction \mathbf{r} "on the fly."

To execute the instruction, we need the desirable (and fixed) number of nodes m and the search direction \mathbf{r} . The former results in the steplength for the guess point, the latter in the direction of the corrector to the NT (modelling the RP). The problems with the choice of \mathbf{r} for finding a special saddle on the NT are discussed below, Sec. V, examples V B and V E. To check the convergence of \mathbf{p} , thus that the projected and inverse gradient \mathbf{g} in Eq. (5) is zero, we also need a convergence criterion ϵ .¹ (Note that \mathbf{x}_{ini} and \mathbf{x}_{fin} need not be

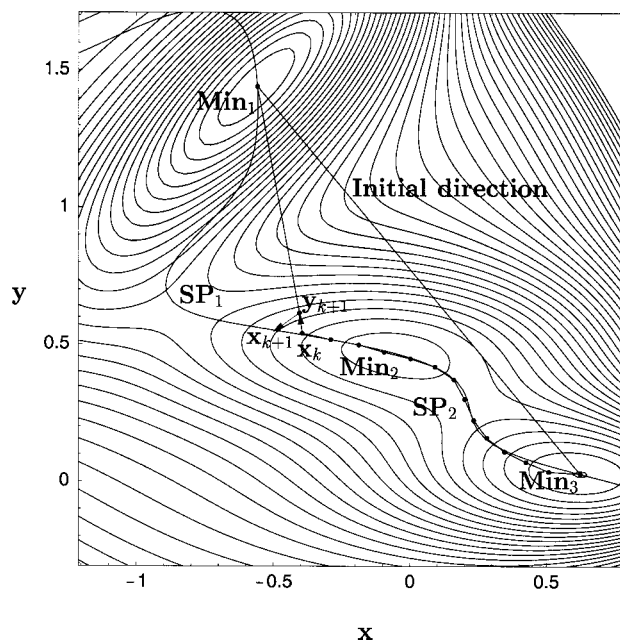


FIG. 1. GS method on Müller–Brown potential from minimum M_3 to minimum M_1 . The predictor step at \mathbf{x}_{13} is shown, and the corrector back to the searched RP (arrows). The desired number of nodes is $L=23$. The Newton trajectory to the initial direction is included for comparison. The growing string follows the NT very well.

minima; they can be any points in two different pockets of the PES which we want to connect by a NT over a SP: choose the gradient in \mathbf{x}_{ini} to be the search direction. \mathbf{x}_{fin} may not be on the NT, however, the SP may be.)

In this paper, we do not reparameterize the string. The NT with respect to \mathbf{r} should also be followed if the nodes increase their distance and are not distributed evenly. If the molecule is described in Cartesian coordinates with three overall rotations, we sometimes meet the problem of a mild "bunching up" of nodes. It is discussed in Sec. IV B below, and in example V E. Generally, we hope for an automatically evenly distributed growing string, which then is an indicator for a well-chosen search direction and a good execution of the corrector.

IV. IMPROVEMENT OF THE PROJECTED GRADIENT SEARCH BY THE CG+ METHOD

The corrector step by Eq. (5) uses a projected gradient, which works well in low dimensions, and which works finely if the PES section of the main direction is not too flat, in relation to further orthogonal directions. However, the steplength of the gradient methods is always a problem. Using a dampening factor η one can, with some experience, successfully apply the steps \mathbf{p} of Eq. (5). One condition is that the tolerance for the corrector is not too sharp! But this is recommendable because we search a coarse approximation of the RP, which should lead over a maximum value of the energy in any neighborhood of the SP. The SP itself can then be improved by another method.

In the general, higher-dimensional case, however, we need improved methods. A minimizer with high merits is the CG+ algorithm of Liu *et al.*¹³ CG+ is a conjugate gradient code used for solving nonlinear, unconstrained optimization

problems. We concentrate on the positive Polak–Ribiere parameter ($\beta := \max\{\beta, 0\}$). The CG+ routine is especially effective on problems involving a large number of variables. It needs the subroutine which, given an input vector \mathbf{x} , returns the function and gradient for the function one wants to minimize. The Hessian is never computed. The steplength along a search direction is additionally determined by a line search routine, which is a slight modification of a routine written by Moré and Thuente.¹⁴ The purpose is to find a step which satisfies a sufficient decrease condition and a curvature condition. If applying the projected and inverse gradient \mathbf{p} of Eq. (5) in the steepest descent search, we go trivially orthogonally to the search direction \mathbf{r} in every step. However, if applying CG+ as a minimization, using the projected and inverse gradient (5) for the input, this does not guarantee that the method moves in the constrained plane orthogonally to the search direction of the Newton trajectory search. We choose a more indirect way to save the orthogonal search to the direction \mathbf{r} .

A. Lagrangian condition

We formally pose an additional degree of freedom to the energy function $E(\mathbf{x})$ by

$$L(\mathbf{x}, \lambda) = E(\mathbf{x}) - \lambda \mathbf{r}^T \cdot (\mathbf{x} - \mathbf{y}) \quad (7)$$

and search a minimum for the (\mathbf{x}, λ) variables, where \mathbf{y} may be the initial point of a corrector loop (see Fig. 1). λ is the Lagrangian multiplier, and the linear equation of a hyperplane

$$C(\mathbf{x}) = 0 = \mathbf{r}^T \cdot (\mathbf{x} - \mathbf{y}) \quad (8)$$

should be fulfilled at the end of the corrector loop, as well as the value of the $(n+1)$ st variable

$$\lambda = \pm \|\mathbf{g}(\mathbf{x})\|. \quad (9)$$

The gradient for L is for the first n dimensions $\mathbf{g}(\mathbf{x}) - \lambda \mathbf{r}$, and the last entry is $-C(\mathbf{x})$. An application of \mathbf{P}_r on the first n dimensions of the gradient of L again results in Eq. (4), and Eq. (3) is fulfilled with ansatz (9). We will find a minimum solution of the constrained problem (7) by employing the known conditions of L directly in a modified, but “unconstrained” CG+ run:

- (i) We modify the procedure, putting for every iteration step the “true” λ value (9) for the input.
- (ii) We use the gradient of $L(\mathbf{x}, \lambda)$ for the CG+ program, however, the calculated steps D_j , $j=1, \dots$ of that procedure are projected by \mathbf{P}_r in every loop (and by \mathbf{P}_{R_X} , \mathbf{P}_{R_Y} , and \mathbf{P}_{R_Z} , see below). Thus, we only use steps in the hyperplane $C(\mathbf{x})=0$.
- (iii) We suppress some strong tests of the CG+ program, for example, we allow that in some steps the search direction is not always a strong descent direction: we leap over the test $D_j^T \cdot \mathbf{g} > 0$. We generally restrict the steplength along a search direction D_j , such as in Ref. 9.

There is some hope that this modified CG+ searches better in the projected subspace orthogonal to \mathbf{r} than the pure pro-

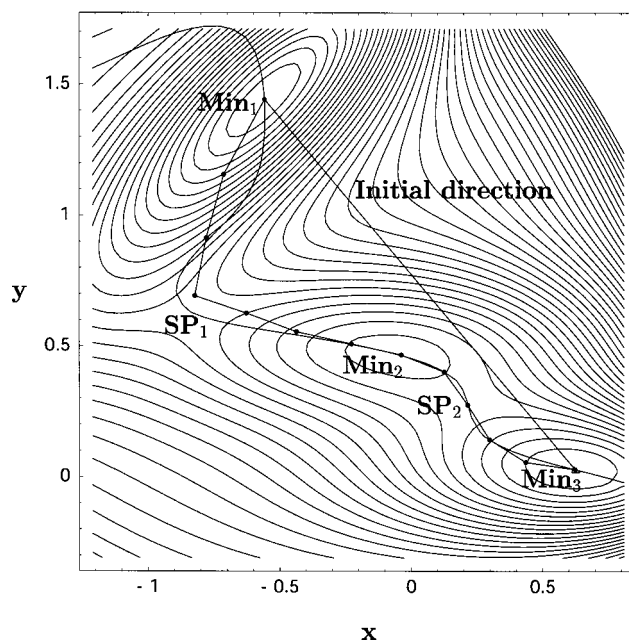


FIG. 2. Reaction path on the Müller–Brown potential from minimum M_3 to minimum M_1 . An 11-node chain is obtained using the Newton projector. The convergence of the growing string method needs the calculation of 19 gradients. The search direction for the GS method is readjusted on the course.

jected gradient \mathbf{p} . An example below needs a very sharp threshold of the corrector: here the modified CG+ works well.

B. Zero eigenvalues

The projected gradient, Eq. (5), contains (usually small parts of) the three directions of the so-called zero eigenvalues of a rotation of the molecule in space, if we work in Cartesian coordinates, and if we are away from stationary points.^{15,16} If the condition for the tolerance of the corrector is not too sharp, then the three components of the gradient, which do not contribute to a descent of the energy, are not of interest. However, in the alanine dipeptide example below, we look for a pathway in a subspace of a very low curvature, in contrast to other degrees of freedom of the molecule. The PES section of the main directions is very, very flat. The norm of the gradient is small, and the steplength of the gradient method has to be very small to avoid zigzagging, thus avoiding the trapping of the iteration near a narrow curved valley. Here, the threshold of a corrector step has to be sharper than the “zero” part of a whole rotation.

Executing the process of minimization steps along dampened vectors \mathbf{p} of Eq. (5), there emerges a strange process of a kind of redistribution of steps into the directions of the molecule’s rotation. This even happens if the linear hyperplane equation $C(\mathbf{x})=0$, Eq. (8), is fulfilled throughout in all corrector loops (for example, with $\pm 1.0E-10$ deviation). The redistribution leads to a gliding down of the optimized point. It moves down in the reaction valley nearer to the local minimum, being the start or end point of our reaction path. Thus, we lose the advantage of the NT method, not to

need spring forces of a chain of points.¹ In mathematical test problems without “nonlinear zero directions” one does not find such a redistribution.

Modern quantum codes should be sufficiently reliable such that the computed gradient is at least rotationally invariant, so if one were to explicitly project rotations out of the gradient vector, it would be unchanged. However, this is not the case. The rotations of the whole molecule play a role here, under the use of many small-gradient steps. In the first order, one can even project out the linear components of the rotational parts of the gradient,¹⁷ however, it is only a shift of the problem to lower figures. Nevertheless, we use this projection for the directions D_J , which are given by the CG+ method. With $J=3(I-1)$ for $I=1, \dots, n/3$, we define the three rotational zero directions

$$\begin{aligned} R_X(J+1) &= 0, & R_X(J+2) &= -X(J+3), \\ R_X(J+3) &= X(J+2), \\ R_Y(J+1) &= X(J+3), & R_Y(J+2) &= 0, \\ R_Y(J+3) &= -X(J+1), \\ R_Z(J+1) &= -X(J+2), & R_Z(J+2) &= X(J+1), \\ R_Z(J+3) &= 0, \end{aligned} \quad (10)$$

and use, after a normalization, the three vectors \mathbf{R}_X , \mathbf{R}_Y , and \mathbf{R}_Z in a projection operator $\mathbf{P}_{\mathbf{R}_X} \cdot \mathbf{P}_{\mathbf{R}_Y} \cdot \mathbf{P}_{\mathbf{R}_Z}$ in analogy to the $\mathbf{P}_{\mathbf{r}}$ projection (2).

V. EXAMPLES

A. Müller–Brown PES

We use the Müller–Brown (MB) PES,¹⁸ see Fig. 1, for a test of the pure Newton projector with the growing string method. We start at M_3 with a straight line between the two outer minima, M_3 and M_1 . It is the initial search direction \mathbf{r} . We use the dampening factor of $\eta=0.13$, and the same convergence criterion of $\epsilon=0.08$ for the coarse convergence of the loop of the actual guess point. A chain of $m=11$ nodes is used in Fig. 2 to illustrate the result. (The slight corner cutting is due to the coarse tolerance value.) In Ref. 1 we needed $k=9$ loops for the whole test chain, thus, the number of gradients needed was km . However, here, we move every new guess point in its own loop. Note that the guess point is already near the RP: usually, the convergence of the corrector needs one or two steps. The dampening factor η can vary; downwards it can be as small as one wants, however, going to higher values, it is restricted by the zigzagging of the algorithm. Of course, if it is smaller, we have to execute more steps.

Because the saddle point SP_1 is far away from the starting chain, we may additionally use a moderate turn of the search direction along the string. If the actual node number k surpasses half of the chain length $L/2$, we take for \mathbf{r} the direction of node $(k-L/2)$ to the final minimum M_1 . Figure 3 shows the effort for different chain lengths. The effort increases quite linearly in the number of nodes from nine gra-

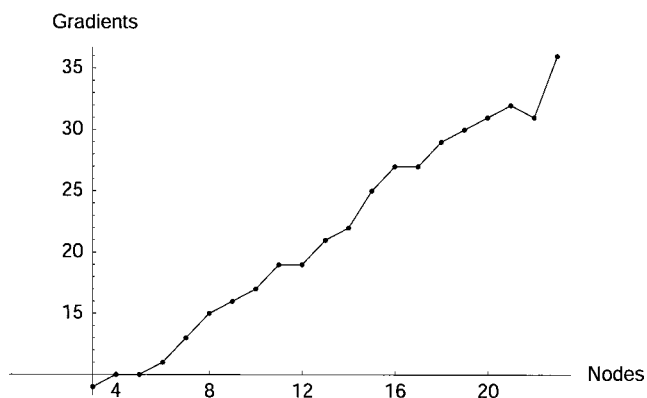


FIG. 3. Effort of the growing ends string method for the MB potential.

dent calculations, which we need for three nodes, to 36 gradients for 23 nodes. The improvement against the moving of a full initial chain¹ is dramatic, as well as the saving against the growing string method for the steepest descent pathway,² where the effort is between 100 and 40 gradient calculations. (But in that method the computational effort scales much better with the number of nodes.) In Ref. 9 there are around 500–1000 gradient calculations used for a 17-node nudged elastic band on the MB surface (Figs. 4 and 5 of Ref. 9).

B. Four-well potential

Figure 4 shows further a two-dimensional (2D) model. It is the slightly changed function for a four-well potential¹⁹

$$E(x,y) = x^4 + y^4 - 2x^2 - 4y^2 + xy + 0.3x + 0.1y. \quad (11)$$

Again, we look for a RP from M_3 to M_1 . The RP calculated has to connect an intermediate minimum. The search has to lead from an initial minimum to the intermediate over the first SP_2 , and then over the second SP_1 to the final minimum. A taut chain of points may lead from M_3 over the highest SP_1 to M_1 , surrounding only the summit near (0,0).

Figure 4(a) demonstrates a possible drawback of the NT method: the search direction \mathbf{r} (here the direction from M_3 to M_1) may not be defined cleverly. If there are more than two minima we, *a priori*, cannot know which search direction leads to a close, desired connection between the stationary points. Beginning at M_3 , the NT to \mathbf{r} leads correctly to SP_2 , further to M_2 , and further to SP_1 . However, from SP_1 , the NT leads to the summit of the surface, but not directly to the final minimum. The approximation by a growing string method with projector (5) leads very quickly, and correctly, up to SP_1 , but then it skips downhill to a next section of the NT.

In Fig. 4(b) we again change the search direction on the fly. The search direction \mathbf{r} becomes the actual direction between the last node and the final minimum. Clearly, such a definition is better adapted to complicated PESs.

C. Lennard-Jones cluster LJ_7

Next, we take the Lennard-Jones cluster²⁰ for seven argon atoms, LJ_7 ,^{1,9,21} for a 21-dimensional (21D) application of the growing string method with the Newton projector. There are two minima, a pentagonal bipyramid at -16.51

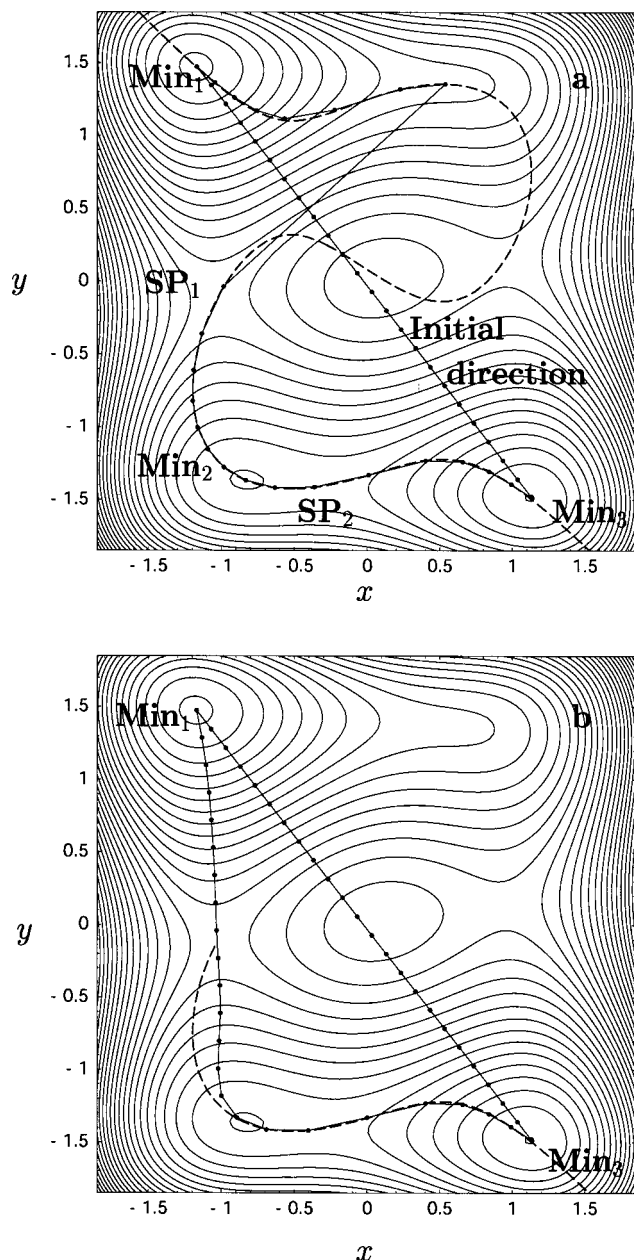


FIG. 4. Newton trajectory (dashes) and the growing ends string method (connected bullets) for a four-well potential including an initial chain, for comparison. (a) The fixed search direction between both minima is not well chosen; for the second part of the RP, see text. (b) The search direction for the GS method is readjusted on the course.

energy units and a capped octahedron at -15.94 energy units. The search direction \mathbf{r} is the direction between the minima. The straight line guess between the minima are the three-dimensional (3D) coordinates (x,y,z) of atoms 1–7 of the two minima in the linear interpolation (6).¹ We use the small dampening factor of 0.03, corresponding to the higher dimension of the example.¹ A tolerance of $\epsilon=0.06$ works for the convergence of the projected gradient norm of every loop. A chain of 12 points is used, and the string method with projector (5) results in the RP over the known SP of -15.44 energy units with 12 gradient calculations. In Ref. 1 we needed $k=10$ loops. It is a saving of gradient calculations of an order of magnitude over Ref. 1. A test is reported with a

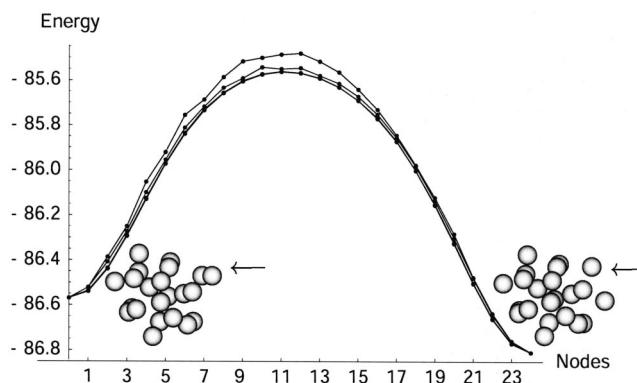


FIG. 5. Growing ends string method with 23 nodes for the LJ_{22} potential (assuming argon). Shown is the energy profile. The left arrows indicate the two outmost right atoms which are mainly involved in the rearrangement. From top to bottom, the resulting curves for the corrector thresholds $\epsilon=1.0, 0.5$, and 0.1 are shown. The SP at node 11 is well approximated.

7-node chain,⁹ where the result begins at about 50 gradients (Fig. 6 of Ref. 9). We need, for seven nodes, only seven gradient calculations with the same parameters 0.03/0.06 as above.

The PES of the LJ cluster is used in the full Cartesian coordinates, including the possibility of overall translation and rotation of the cluster. Here it does not mean any difficulties for the method, because the downhill steps of the projected and inverse gradient \mathbf{p} mainly use the very large nonzero parts of the gradient of the true internal coordinates, in comparison to the nonzero parts of the rotational directions.

Note that the search directions between permutational rearrangements such as in Ref. 9 are usually misleading because there the \mathbf{r} depicts a pathway into the high-energy regions, or the calculation diverges. The GS-NT method may have trouble with such minima, may be no direct neighbors on the PES. However, usually, if the evolving end of the string is far away from the starting chain, the search direction may be additionally adapted to the direction between the actual node and the end minimum.

D. Lennard-Jones cluster LJ_{22} and the CG+ method

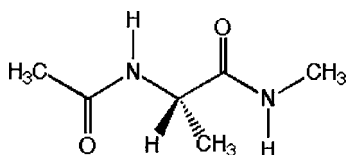
For an exercise in front of the alanine dipeptide example below, we treat the toy problem of the LJ_{22} cluster of an analogous dimension, and apply the CG+ method including the projection of \mathbf{P}_r and of the rotational directions (10). The result of the test is given in Fig. 5, where we use the global minimum of that cluster from the Wales tables,²² at the right hand side, and a neighboring second-lowest-energy minimum being only slightly higher in its energy. A chain of 23 nodes is used. The starting chain is again the simple linear combination of the two minima in Cartesian coordinates. Four successful runs are done with one different parameter, the threshold $\epsilon=1.0, 0.5, 0.1$, and 0.05 , now for every gradient component. The CG+ method needs 56, 100, 212, or 328 gradient calculations, respectively. However, for $\epsilon=0.01$ the optimization degenerates due to the overall rotation of the molecule (Sec. IV B), although we apply the projections

$P_{RX} \cdot P_{RY} \cdot P_{RZ}$. The threshold is too “sharp” for an exploration of the PES in Cartesian coordinates.

The steplength of the CG+ method is optimized in the algorithm. We need not give this parameter—and it is generally higher than the value being maximally possible under the pure projected gradient method. Here we generally restrict the steplength by 0.12 units because the LJ potential is very rugged, cf. Fig. 5 of Ref. 23. In Fig. 5 the last two runs cannot be distinguished, they coincide in the graphics. The highest point of this lowest profile is exactly the SP of a rearrangement of the cluster. Also the first test with the coarse $\epsilon=1.0$ results in a good estimate of the SP. The 56 gradients, which one needs in this most optimistic run, are less than the dimension of the problem. It means 2–3 gradients per node. The calculation of the LJ₂₂ energies and gradients in such a number only takes up a few seconds using a personal computer (PC).

E. Alanine dipeptide

The determination of RPs in polypeptides (protein folding) has become a terrifically vibrant field of inquiry. But for large peptide systems, we are still limited to the determination of one or a few RPs from a given minimum to another one. Which one is the global minimum energy path (MEP)? We do not know! If a search direction is chosen, and if the search is successful, we will obtain a “local” MEP. If the SP of the path is sufficiently low, then the path may be the global MEP between the minima.²⁴



A common benchmark molecule for testing protein modeling algorithms is alanine dipeptide, which is formed by condensing the amino acid alanine $H_2N-CH(-CH_3)-COOH$ with a CH_3-COOH at its amine end and a H_2N-CH_3 at its carboxyl end, in order to mimic the two-peptide-linkage environment in which alanine is found in proteins. We use the example of the 66-dimensional alanine dipeptide for a rearrangement between the minimum C5 and the C7_{ax} minimum or vice versa.^{2,25} It is mainly a rotation along the (Φ, Ψ) angles from $(-170, 170) = (190, -190)$ to $(75, -60)$ set of values of the backbone dihedral angles Φ (C–N–C_α–C) and Ψ (N–C_α–C–N). C_α is the central C atom in Scheme 1. Both structures are “sheets” because it is $|\Phi + \Psi| < 30^\circ$. The rearrangement goes through a SP region with $\Phi + \Psi < -50^\circ$, representing a “right-handed helix.” The C7_{ax} minimum seems to be in a single bowl of the PES, where the C5 belongs to a wider deep pocket containing further minima such as C7_{eq} and α_R , compare Fig. 1 of Ref. 26 or Fig. 2 of Ref. 27. However, between both is a 2D hill in a (Φ, Ψ) map.

The straight line guess between the minima are the 3D coordinates (x, y, z) of atoms 1–22 of the two minima in the linear interpolation (6). Of course, the linear interpolation of the two conformers in Cartesian coordinates, for a guess² of the RP of alanine dipeptide, is very coarse. So to say, it is a maladroit choice. One ignores the curvilinear behavior of the

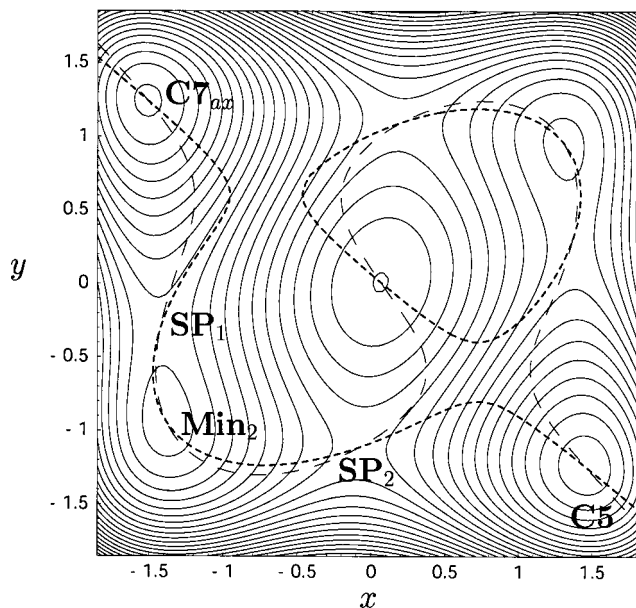


FIG. 6. Two Newton trajectories for a four-well potential with minima C5 and C7_{ax}. Thin long dashes: NT to search direction between both minima. (It is not well chosen.) Short bold dashes: The search direction for the NT is well adapted to connect the C5 and C7_{ax} minima.

two parts of the molecule. For a demonstration of the method, however, guess (6) is a provoking task, a challenge. The growing string method avoids the very unrealistic structures of the “molecule” on the linear interpolation pathway. There the energies would be extremely high, some hundreds to thousand kcal/mol, where, on the possible rearrangement path, the SP is in the range of 9.5 kcal/mol above the lower minimum C5.

We use the 3–21G level of computation. The example has a further drawback: the RP between the minima C5 and C7_{ax} is a combined RP. There an intermediate minimum exists in between, and there two SPs exist between the minima C5 and C7_{ax}. (Compare Fig. 1 of Ref. 26, or the model in Fig. 6. It may be that the intermediate flattens out under a high-level quantum mechanical calculation,²⁸ or that the minimum is nearly unstable,²⁷ and a frequent transition occurs from it to the more stable minimum C7_{ax} in the neighborhood.) A method for a “pure” RP search, in any definition, has to detect the intermediate. Thus, our GS method for NTs has to detect this problem, if the search direction is well adapted.

To explain the problem of the search direction, as well as a brief motivational journey, we chose a test potential. Figure 6 simplifies the alanine dipeptide rearrangement from C5 to C7_{ax} structure. The 2D model¹⁹ is adapted to the 2D (Φ, Ψ) section of the 66D configuration space (or the 60D in internal coordinates). It is the function

$$E(x, y) = x^4 + y^4 - 4x^2 - 2.5y^2 + xy + 0.5x. \quad (12)$$

The (x, y) coordinates may be related to (Φ, Ψ) coordinates by

$$\Phi \approx (x + 3)45^\circ, \quad \text{as well as } \Psi \approx (y - 3)45^\circ.$$

The minimum top left corresponds to C7_{ax}, while the minimum bottom right corresponds to C5.^{26,27} The intermediate

corresponds to the structure α_D in the C5/C7_{ax} convention. The growing string should lead from an initial minimum to the intermediate over SP₂ (it is SP₁₃ in Ref. 27), and then over the second SP₁ to the final minimum. Note that the routes from C5 to C7_{eq} to α_R/α_L ,²⁹ and then to C7_{ax},³⁰ are not treated here. Also the route from C5 to the intermediate top right in Fig. 6 is not treated.

For Fig. 6 we use two search directions. The NT with long dashes is the curve $1.3E_x+1.5E_y=0$; that with small, thick dashes is the NT $E_x+1.7E_y=0$. The NT with long dashes is the one with the original direction between the two outer minima. It is not a clever choice to search the RP from M_3 to SP₂. In contrast, the NT leads to the other northern SP of no interest here, and quite worse, after the next SP, it leads to the 2D summit. However, the second NT follows an acceptable search direction. In the next calculations of the real 22-atomic molecule alanine dipeptide, for nodes_{ax} larger than three we use the turn of the search direction after-refined to the direction of (node-3) to final minimum.

In the tests of the GS-NT method with alanine dipeptide, we interface the GS parts with GAUSSIAN03 (Ref. 31) calculations. Energies and gradients are calculated with the 3-21G basis set. (The simple basis is only employed for a model PES. It is obvious that the quantum chemical level used is not sufficient to give a PES of alanine dipeptide, which is correct in all details. It is not the objective of this paper to give a highest-level description of the PES of alanine dipeptide.) The program parts of GS communicate under a shell script, see below Sec. VI. A first series of computational tests are done with the corrector descent along the projected and inverse gradient (5). The predictor step may be given by (6), and the initial chain is between the C5 and the C7_{ax} structure of alanine dipeptide.

In contrast to the LJ₂₂ example above, the alanine dipeptide example is a different story. The projected gradient descent comes to its borderline here. Some results are illustrated in Fig. 7. The general step length for the corrector steps has to be dampened by a value of 0.6, because for a higher value the algorithm runs into an uncontrollable zigzagging. With a value of $\eta=0.575$, we have found a nice, continuous decrease of the energy in every corrector step.

(a) The optimistic test: we chose $\epsilon=0.008$ and 13 nodes between C5 and C7_{ax}. The norm of the reduced gradient will be accepted if it is smaller than ϵ , or if we have done a maximum of 55 corrector steps. In sum we need 604 gradient calculations for curve (a). The ϵ seems still a little too coarse, however, starting at the point with maximum energy of the chain obtained, one may execute the Broyden optimization of the GAUSSIAN03.³¹ It is done by the following commands.

Scheme 2 SP search in GAUSSIAN03 by Broyden's method.

```
$RunGauss
# scf=direct 3-21G opt (ts, saddle=1,
CalcFC,noEigenTest) optcyc=99 test
```

which are followed by the geometry of the node. It leads to the SP₂ after 70 steps. The SP₂ has an energy of $-490.103\ 602$ a.u. and it is situated at $(\Phi, \Psi)=(107.8^\circ, -180.7^\circ)$. [In the 6-31G* basis set, the SP can then be found at $(\Phi, \Psi)=(113.2^\circ, -146.4^\circ)$.] The neighboring points of the chain of (a) lead to the intermediate minimum with an energy

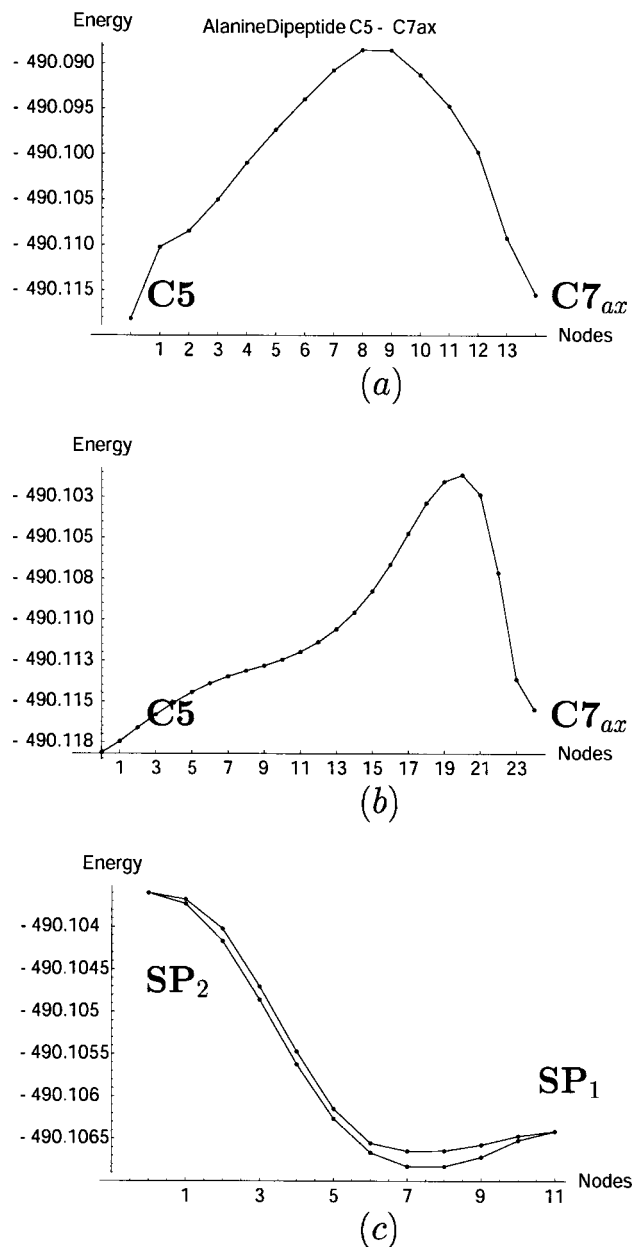


FIG. 7. Approximation of Newton trajectories for alanine dipeptide between the C5 and C7_{ax} minima, see text. Method: projected and inverse gradient [Eq. (9)] dampened by η . The search direction \mathbf{r} for the NT is the direction from start to finish, and after three steps the corresponding direction from former chain points to finish. Shown is the energy profile in a.u. (a) $\eta=0.56$, $\epsilon=0.008$, maximal 55 steps per node. (b) $\eta=0.575$ and ϵ is so small that 151 steps per node are used. (c) NT between the two SPs, $\eta=0.55$, and $\epsilon=0.0013\ 3$ for the upper, as well as $\epsilon=0.0005\ 5$ for the lower curve, maximal 151 steps per node.

of $-490.107\ 274$ a.u. at $(\Phi, \Psi)=(64.3^\circ, -171.8^\circ)$ and to the SP₁, with an energy of $-490.106\ 4$ a.u. at $(\Phi, \Psi)=(61.5^\circ, -127.3^\circ)$ in the 3-21G basis.

(b) The pessimistic test: in a contrary ansatz to (a), we use $\epsilon=0.000\ 5$ and 23 nodes between C5 and C7_{ax}. The maximally allowed corrector steps are now 151. The ϵ is so small that we cannot remain under it, and we cut the corrector in every step at the point after 151 steps. In total we need 23×151 gradient calculations for curve (b). The negative dent in the shape of the curve probably indicates the problem of the zero eigendirections of the molecular rotation: in every

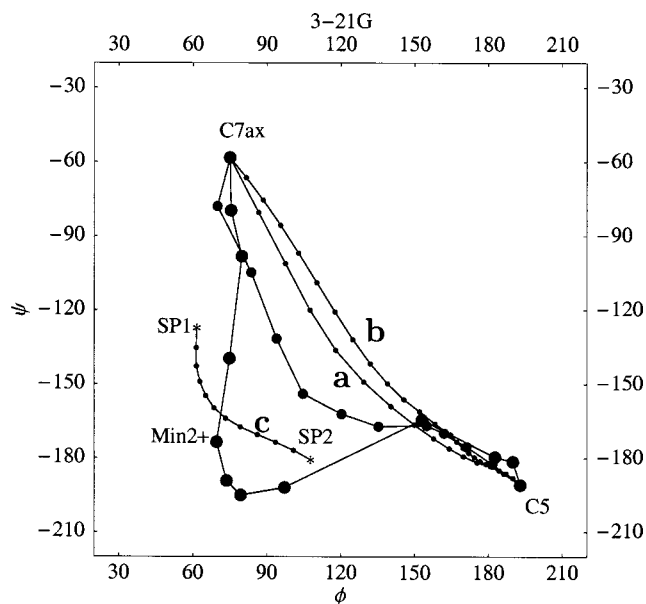


FIG. 10. Approximation of Newton trajectories for alanine dipeptide between the minima $C7_{ax}$ and $C5$, see text. Methods: projected and inverse gradient (thin points) starting at $C5$, and modified $CG+$ optimization (thick bullets) starting at $C7_{ax}$. The two coordinates (Φ, Ψ) of the 60D internal coordinates are shown in a Ramachandran diagram, with adapted axes to the searched reaction pathway. The projected gradient paths correspond with the profiles (a), (b), and the lower curve of (c) of Fig. 7. The connected bold points correspond with the $CG+$ results of Fig. 9. The “better” one (more left and below) is for $\epsilon=0.001$; it is the lower curve of Fig. 9. The other chain of points belongs to $\epsilon=0.0075$. The two SPs (*) and the intermediate minimum (+) are included.

step the system point moves down a very small piece into a reaction valley to the start or final minimum. The nodes mainly concentrate near the initial minimum; for the remainder of the reaction path there are not enough nodes. The profile passes very near the SP_2 energy but nearly all nodes seem to be before the maximum value, and the profile is by no means equidistantly distributed. Starting at the node near the maximum value, with number 21, we get the SP_2 by Berny optimization in 77 steps. Note that the Berny optimization process needs an approximated first eigenvalue of the Hessian of a negative signature. It is fulfilled for points in the upper concave region of the profile. The long optimization way is somewhat surprising if one observes the near equivalence of the SP energy and the energy of the highest string node. Looking at Fig. 10, however, offers the speculation that node #21 is far away from SP_2 . So, indeed, starting at the nearer node #17 one already obtains the SP_2 in 63 Berny steps.

(c) The SPs obtained from curves (a) or (b) are used to start a further NT search for a connection curve in between. Two results are shown in case (c) in Fig. 7. The lower curve is searched with the threshold $\epsilon=0.0005$ and a maximum of 151 steps (which is often exhausted). The curve indicates the intermediate minimum, but does not reach it. The upper test is done with $\epsilon=0.0003$ and 151 maximal steps (which is three times exhausted). It results in a quasimonotonically decreasing curve. (Not shown: if using $\epsilon=0.008$, then the test does not need more than 16 steps per corrector; however, it does not indicate the intermediate minimum. This ϵ is too large, at all.)

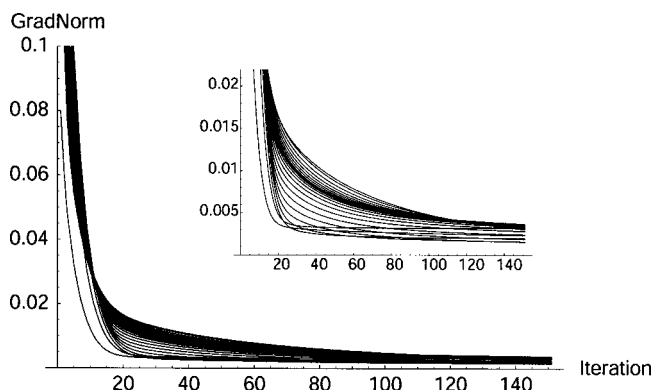


FIG. 8. Convergence history for curve (b) of Fig. 7 for the norm of the projected gradient. In the inlay, curves of nodes 2 to 23 count from top to bottom.

To further understand the influence of ϵ , we show in Fig. 8 the norm of the reduced gradient of curve (b) of Fig. 7 along the corrector loops. Formally, at first view, one could conclude that below the 0.02 threshold a continuation of the corrector loops is useless. However, test (a) demonstrates that the very small threshold of 0.008 may still be too large for a good insight into the PES for a good description of the PES valley by the NT. The growing string construction needs good points of the corrector near the searched NT, at every node. Any single deviation of one node causes a deviation of the following chain because of the use of an after-refining of the search direction.

The way out of the dilemma is a better descent routine, which we have found in the $CG+$ method.

Figures 9 and 10 show the results of the $CG+$ calculations. The ϵ is used now to prove the smallness of every component of the gradient of the Lagrangian ansatz (7). The steplength for the corrector steps is restricted by a value of 2.5 units. Note that we additionally have changed the order of the two minima: we start with minimum $C7_{ax}$ and search a growing string to the $C5$ minimum. The reason is that we thus meet the lower SP_1 first. We use 10 nodes.

(i) The pessimistic calculation of alanine dipeptide: The lower, two hump curve in Fig. 9 is calculated with threshold

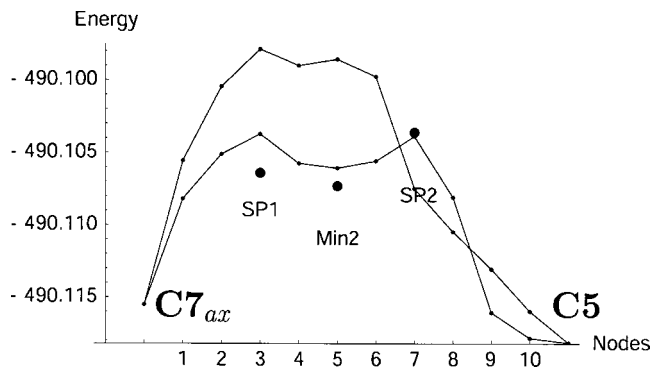


FIG. 9. Approximation of Newton trajectories for alanine dipeptide between the minima $C7_{ax}$ and $C5$, see text. Method: modified $CG+$ optimization. The search direction \mathbf{r} for the NT is the direction from start to finish, and after three steps the direction from former chain points to finish. The energy profile is shown in a.u. The lower curve is for $\epsilon=0.001$ (max 134 steps per node: which were used throughout) and the upper one is for $\epsilon=0.0075$. The energies of the SPs and of the intermediate minimum are included.

$\epsilon=0.001$ for every component of the gradient, and a maximum of $2(n+1)$ steps per corrector. The maximal number of steps is throughout exhausted. The curve shows a double-hump shape. The profile is a very good approximation of a RP between the three included minima, and the two SPs in between. In sum it needs 1340 gradient calculations. One small error is still the large slide down after the SP_2 , which may be caused by the remaining nonlinear parts of the zero directions of a molecular rotation (the ϵ is already too small), Or the pattern of Fig. 4(a) plays a role here. If we start an optimization by the BERNY process of GAUSSIAN03 (Ref. 31) at the first maximal node, #3, it needs 34 steps to converge to the flat SP_1 , and using the second maximal node, #7, it needs seven steps to converge immediately to SP_2 .

(ii) The optimistic calculation of alanine dipeptide: The upper curve in Fig. 9 is calculated with threshold $\epsilon=0.0075$ for every component of the gradient. The maximum of $2n$ steps per corrector is never exhausted. The profile is not well adapted to the complicated situation of two SPs and an intermediate. But the profile is still a usable approximation of a RP between the start and final points. Note that the first SP is indicated by a maximum value of energy, however, the second SP is not. In sum the run needs 816 gradient calculations.

Figure 10 depicts the two coordinates of interest, (Φ, Ψ) , of nodes of some of the calculated RPs. The thin points correspond to the corrector calculations by the projected gradient only, where the fat points are CG+ calculations. It is especially clear from such a 2D section that the pure projected gradient here is not the method which results in the searched RP. It is too expensive and too unexact. Looking at the relation between chains (a) and (b), in contrast, indicates that the “sharper” search for (b) results in a worse approximation. The modified CG+ method, however, gives a good image of a possible RP.

Figure 11 proves this: because we now know the existence of the intermediate minimum, we may use it in a last control calculation. We approximate in one run the NT to the direction between the C5 and the intermediate minimum, and start there, in a second run, to approximate the NT to the direction between the intermediate minimum and minimum C7_{ax}. Thus, we turn again the direction of the GS development and start with C5. For the corrector we use the modified CG+ optimization. Ten nodes are fixed for every string and the convergence condition of the corrector is $\epsilon=0.005$ for the stronger slopes on the first pathway, and $\epsilon=0.00333$ for the second pathway. Both values are between the cases used in Fig. 9. The CG+ needs 540+420 gradient calculations, correspondingly. Let us mention that the two GS-NT calculations need 9.6 h using GAUSSIAN03 for energy and gradient at an Itanium[®]2 processor-based HP workstation. Most corrector loops converge on both pathways, with less than 50 steps. (With exceptions: sometimes the convergence is complicated by the coupling of the turning of the flat Φ or Ψ to the very flat internal rotation of a methyl group.) We are compelled to emphasize that the approximations obtained seem to be perfect RPs. The mild edge at node 3 on the first pathway may be a shoulder of the PES.

A shortening of the calculation of a RP approximation of

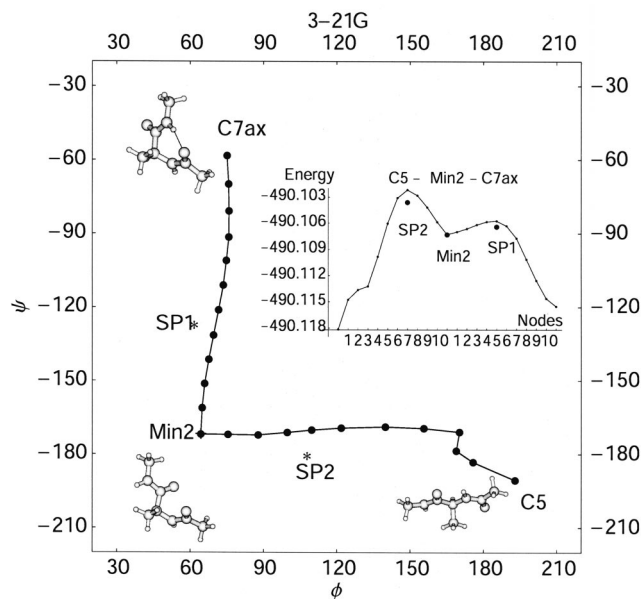


FIG. 11. Approximation of two NTs for alanine dipeptide between the C5 minimum and intermediate minimum, Min_2 , and from there to the minimum C7_{ax}, as well. Method: modified CG+ optimization. Two coordinates (Φ, Ψ) are shown in a Ramachandran diagram. Ten nodes are used for every string, and thresholds $\epsilon=0.005$ and 0.00333 , respectively. The inlay shows the energy profile of both paths in the order of their calculation.

alanine dipeptide is to obtain by other predictor steps. ϕ is the single coordinate which changes along the RP from C5 to M_2 . Using Cartesian coordinates, the singular position of ϕ is hidden by a complicate, however, unnecessary nonlinear coupling. If one transforms the point \mathbf{x}_k (on the RP) into a z -matrix representation including ϕ , and if one also transforms the point M_2 using the same z -matrix, then one can use the linear combination of Eq. (6) for the z -matrix coordinates of \mathbf{x}_k and M_2 . Naturally, nearly all z -matrix coordinates coincide, but the ϕ coordinate differs for the two points \mathbf{x}_k and M_2 . Naturally, the next predictor for \mathbf{y}_{k+1} under Eq. (6) then gives a better point being nearer to the searched RP. The \mathbf{y}_{k+1} is transformed back to Cartesians, and the corrector loop can start as in the former calculations.

Applying this strategy, we need less nodes of the chain over the SP, and we can raise the threshold ϵ . We needed in four test calculations with five nodes only the following numbers of gradient calculations, for the RP $C5 \rightarrow M_2$: the run $\epsilon=0.005$ needs 141 gradients, $\epsilon=0.0075$ needs 87 gradients, $\epsilon=0.01$ needs 57 gradients, and the run $\epsilon=0.02$ needs 21 gradients. The RP approximations obtained cross the SP region of SP_2 very well, they are comparable to the case of Fig. 11, and the highest point also meets the SP well, for the first three approximations, see Fig. 12.

VI. IMPLEMENTATION OF CG+ AND GAUSSIAN03 FOR THE GS METHOD

We use a script to call the GS-NT method in modular form, including the CG+ corrector, and to call the energy and gradient in an independent program. First, we describe the script for LJ₂₂.

Scheme 3 Shell script for an LJ₂₂ cluster: Calculation of NTs

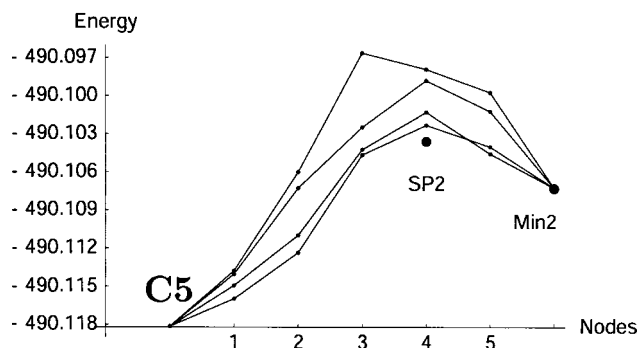


FIG. 12. Approximation of four NTs for alanine dipeptide between the C5 minimum and Min_2 . Method: modified CG+ optimization. The linear combinations of coordinate Φ are used for predictor steps, and five nodes are calculated for every string. The thresholds are $\epsilon=0.005, 0.0075, 0.01$, and 0.02 from bottom to top.

```
call startGS with initialization
call energy
call projector
call predictor
export status=0
while (test $status -ne 10) do
call projector
call energy and gradient
call corrector: new GS point, test
export status=$?
if (test $status -eq 1)
then
call predictor
export status=$?
fi
done
exit
```

The procedures are in FORTRAN and they are used with a G77 compiler on a PC with a LINUX operation system. Dimension and thresholds are put in the programs. The variable *status* controls the interplay between the parts predictor or corrector. The procedures can be downloaded.³²

We use the GAUSSIAN03 (Ref. 31) in an analogous modular partition of GS-NT. We need the *input* file for every current geometry. The file *oben* contains the Gaussian command line for the used *input* file; the lines are:

Scheme 4 Head of GAUSSIAN03 input for corrector steps (file *oben*).

```
$RunGauss
# scf=direct 3-21G opt optcyc=1 test
```

which are followed by comment lines and the actual geometry of the molecule in Cartesian coordinates; it is given by file *AlaPointG*. The GAUSSIAN03 calls *input* and gives *output*. From the use of the GAUSSIAN03 we need the energy and gradient of the current point, which we extract from the file *output*; it is done by some commands of the script.

Scheme 5 Shell script for the alanine dipeptide molecule: Calculation of NTs

```
call startGS: initialization
cat oben AlaPointG > input
```

```
call gaussian03
grep 'SCF Done: E' output > energy
tr -s ' ' < energy > entr
cut -d' ' -f6 entr > energy
grep 'SCF Done: E' output > ALAenergy
grep D13 output | grep estimate > ALAd13
grep D27 output | grep estimate > ALAd27
call projector
call predictor
# GS cycle
export status=0
while (test $status -ne 10) do
cat oben AlaPointG > input
call gaussian03
grep 'SCF Done: E' output > energy
tr -s ' ' < energy > entr
cut -d' ' -f6 entr > energy
grep -n 'Axes restored to original' out-
put | head -n 1 >noline
cut -d':' -f1 noline > num
head -n $num output |tail -22 >grad
call corrector: new GS point, test
export status=$?
if (test $status -eq 1)
then
grep 'SCF Done: E' output >= ALAenergy
grep D13 output | grep estimate >= ALAd13
grep D27 output | grep estimate >= ALAd27
call projector
call predictor
export status=$?
fi
done
# end GS cycle
exit
```

The program parts are startGS, projector, corrector with modified CG+, and predictor. They communicate via data files. The procedures are in FORTRAN and they are used with an F90 compiler. The procedures can be downloaded.³² The PES calculation is executed here by the Gaussian program. The diverse *grep* commands and the following lines are used to extract the energy and the Cartesian gradient from the Gaussian *output*, as well as the (Φ, Ψ) pair of dihedrals, D13 and D27.

VII. DISCUSSION

The user of the string method for NTs must supply the gradient, but knowledge about the Hessian matrix is not required. Using the final minimum (or a point in the aim pocket of the PES) for the guiding star replaces all traditional efforts for the tangent calculation in a predictor step. The Newton projector (5) allows that every point of an actual string over the PES can move locally and independently

from the other points of the string to its final place on the NT.¹ It makes the Newton projector in a special kind very well adapted to the growing string idea.

How to thread a string through the eye of the PES, the SP? Per definition, a RP leads over the SP, and we automatically obtain the SP if we are able to calculate the whole RP by a chain of points. In this work we construct the RP by a NT to provide SP candidates for further refinement. Starting from the known minima, we use the growing string along a NT as a model of the RP. We search with a projector defined by search direction \mathbf{r} , for a example, by the direction between the two minima. The projector (5) works well for the first steps of the corrector loop. We avoid the zigzagging of the modified gradient steps (5) if we use a coarse tolerance. The alternate use of the conjugated gradient (CG+) method¹³ for the corrector is tested for the alanine dipeptide example, where the modified gradient steps (5) alone are not effective. The GS-NT method scales well with the size of the system and the number of nodes of the string.

In addition to the projection of the search direction, the linear parts of the molecular rotations are also projected out. If one works in Cartesian coordinates, then one includes external rotations of the molecule. Then the choice of the convergence criteria ϵ plays a crucial role in the quality of the result, where ϵ has to be a small enough threshold. However, it must not be too small. A successful interval for ϵ depends on the PES and has to be found out by trial and error.

The search of the corrector is done orthogonally to \mathbf{r} by a Lagrangian formulation. The CG+ is used like an unconstrained optimization method,¹³ however, inside CG+, the calculated corrector direction, D_j , is projected in every step. The CG+ is coupled with an effective line-search routine.^{13,14}

The search direction \mathbf{r} , itself, works well if there is a valley to the SP searched on the whole.³³ If we are in such a valley, then an after-refining of the search direction “on the fly” is a good device. Note that near to a valley floor many different NTs “concentrate”.^{34,35} Then the GS-NT method is stable regardless of the initial guess of \mathbf{r} .

Like the intrinsic reaction coordinate (IRC), the steepest descent from SP, most of the NTs can serve as a model of a RP.^{34,35} Thus, the calculation of NTs may be a serious alternative to the IRC using the growing string method. The growing string procedures described can be downloaded.³² (Note that the implementation of an algorithm is more important than the algorithm itself.)

ACKNOWLEDGMENTS

The work was made possible through the financial support of the Deutsche Forschungsgemeinschaft, and through the computer time of the University of Leipzig. The author especially thanks Professor Dr. H.-J. Hofmann from the In-

stitute of Biochemistry, University Leipzig, for giving him an introductory lesson into the model world of alanine “dipeptide.”³⁶

¹W. Quapp, *J. Comput. Chem.* **25**, 1277 (2004).

²B. Peters, A. Heyden, A. T. Bell, and A. Chakraborty, *J. Chem. Phys.* **120**, 7877 (2004).

³M. Hirsch and W. Quapp, *Chem. Phys. Lett.* **395**, 150 (2004).

⁴I. H. Williams and G. M. Maggiora, *J. Mol. Struct.: THEOCHEM* **89**, 365 (1982).

⁵W. Quapp, M. Hirsch, O. Imig, and D. Heidrich, *J. Comput. Chem.* **19**, 1087 (1998).

⁶W. Quapp, M. Hirsch, and D. Heidrich, *Theor. Chem. Acc.* **100**, 285 (1998).

⁷S. C. Ammel, H. Yamataka, M. Aida, and M. Dupuis, *Science* **200**, 1555 (2003).

⁸D. A. Liotard and J. P. Penot, in *Study of Critical Phenomena*, edited by J. DellaDora, J. Demongeot, and B. Lacolle, (Springer, Berlin, 1981), p. 213.

⁹S. A. Trygubenko and D. J. Wales, *J. Chem. Phys.* **120**, 2082 (2004).

¹⁰J. M. Anglada, E. Besalú, J. M. Bofill, and R. Crehuet, *J. Comput. Chem.* **22**, 387 (2001); J. M. Bofill and J. M. Anglada, *Theor. Chem. Acc.* **105**, 463 (2001); R. Crehuet, J. M. Bofill, and J. M. Anglada, *ibid.* **107**, 130 (2002).

¹¹W. Quapp, *J. Comput. Chem.* **22**, 537 (2001).

¹²M. Hirsch and W. Quapp, *J. Math. Chem.* **36**, 307 (2004).

¹³J. C. Gilbert and J. Nocedal, *SIAM J. Optim.* **2**, 1 (1992); G. Liu, J. Nocedal, and R. Waltz, CG+ software, <http://www.ece.northwestern.edu/~nocedal/GG+.html>

¹⁴J. J. Moré and D. J. Thuent, *ACM Trans. Math. Softw.* **20**, 286 (1994).

¹⁵A. Guichardet, *Ann. Inst. Henri Poincaré, Sect. A* **40**, 329 (1984).

¹⁶T. Iwai, *Ann. Inst. Henri Poincaré, Sect. A* **47**, 199 (1987); *Phys. Lett. A* **149**, 341 (1990).

¹⁷W. Miller, N. C. Handy, and J. E. Adams, *J. Chem. Phys.* **72**, 99 (1980).

¹⁸K. Müller and L. D. Brown, *Theor. Chim. Acta* **53**, 75 (1979).

¹⁹S. Wolfe, H. B. Schlegel, I. G. Csizmadia, and F. Bernardi, *J. Am. Chem. Soc.* **97**, 2020 (1975).

²⁰J. E. Lennard-Jones, *Proc. R. Soc. London, Ser. A* **106**, 463 (1924).

²¹P. Chaudhury, S. P. Bhattacharyya, and W. Quapp, *Chem. Phys.* **253**, 295 (2000).

²²D. J. Wales and J. P. K. Doye, *J. Phys. Chem. A* **101**, 5111 (1997); <http://www.doye.ch.cam.ac.uk/jon/structures/LJ>

²³W. Quapp, M. Hirsch, and D. Heidrich, *Theor. Chem. Acc.* **105**, 145 (2000).

²⁴H. Liu, Z. Lu, G. A. Cisneros, and W. Yang, *J. Chem. Phys.* **121**, 697 (2004).

²⁵B. M. Pettitt and M. Karplus, *J. Am. Chem. Soc.* **107**, 1166 (1985).

²⁶A. Preczel, Ö. Farkas, I. Jákl, I. A. Topol, and I. G. Csizmadia, *J. Comput. Chem.* **24**, 1026 (2003).

²⁷D. S. Chekmarev, T. Ishida, and R. M. Levy, *J. Phys. Chem. B* **108**, 19496 (2004).

²⁸M. Feig, A. D. MacKerell, Jr., and C. L. Brooks III, *J. Phys. Chem. B* **107**, 2831 (2003).

²⁹C. Guilbert, D. Perahia, and L. Mouawad, *Comput. Phys. Commun.* **91**, 263 (1995).

³⁰E. Neria, S. Fischer, and M. Karplus, *J. Chem. Phys.* **105**, 1902 (1996).

³¹M. J. Frisch, G. W. Trucks, H. B. Schlegel, *et al.*, GAUSSIAN 03, Revision B.03, Gaussian, Inc., Pittsburgh, PA, 2003.

³²W. Quapp, <http://www.math.uni-leipzig.de/~quapp/GS>

³³M. Hirsch and W. Quapp, *J. Mol. Struct.: THEOCHEM* **683**, 1 (2004).

³⁴W. Quapp, *J. Theor. Comput. Chem.* **2**, 385 (2003).

³⁵M. Hirsch, *Zum Reaktionswegcharakter von Newtontrajektorien*, dissertation, Fakultät für Chemie und Mineralogie, Universität Leipzig, December 2003.

³⁶K. Möhle, H.-J. Hofmann, and W. Thiel, *J. Chem. Phys.* **22**, 509 (2001).